

## PAPER

# Smart multi-channel two-dimensional micro-gas chromatography for rapid workplace hazardous volatile organic compounds measurement†

Cite this: *Lab Chip*, 2013, 13, 818

Jing Liu,<sup>ab</sup> Jung Hwan Seo,<sup>bc</sup> Yubo Li,<sup>ad</sup> Di Chen,<sup>ab</sup> Katsuo Kurabayashi<sup>bc</sup> and Xudong Fan<sup>\*ab</sup>

We developed a novel smart multi-channel two-dimensional (2-D) micro-gas chromatography ( $\mu$ GC) architecture that shows promise to significantly improve 2-D  $\mu$ GC performance. In the smart  $\mu$ GC design, a non-destructive on-column gas detector and a flow routing system are installed between the first dimensional separation column and multiple second dimensional separation columns. The effluent from the first dimensional column is monitored in real-time and decision is then made to route the effluent to one of the second dimensional columns for further separation. As compared to the conventional 2-D  $\mu$ GC, the greatest benefit of the smart multi-channel 2-D  $\mu$ GC architecture is the enhanced separation capability of the second dimensional column and hence the overall 2-D GC performance. All the second dimensional columns are independent of each other, and their coating, length, flow rate and temperature can be customized for best separation results. In particular, there is no more constraint on the upper limit of the second dimensional column length and separation time in our architecture. Such flexibility is critical when long second dimensional separation is needed for optimal gas analysis. In addition, the smart  $\mu$ GC is advantageous in terms of elimination of the power intensive thermal modulator, higher peak amplitude enhancement, simplified 2-D chromatogram re-construction and potential scalability to higher dimensional separation. In this paper, we first constructed a complete smart  $1 \times 2$  channel 2-D  $\mu$ GC system, along with an algorithm for automated control/operation of the system. We then characterized and optimized this  $\mu$ GC system, and finally employed it in two important applications that highlight its uniqueness and advantages, *i.e.*, analysis of 31 workplace hazardous volatile organic compounds, and rapid detection and identification of target gas analytes from interference background.

Received 17th October 2012,  
Accepted 12th December 2012

DOI: 10.1039/c2lc41159h

[www.rsc.org/loc](http://www.rsc.org/loc)

## Introduction

Comprehensive two-dimensional (2-D) micro-gas chromatography ( $\mu$ GC) has been under intensive development due to its improved separation capability over 1-D  $\mu$ GC.<sup>1–7</sup> A typical 2-D  $\mu$ GC configuration has two separation columns connected in series with a modulator being installed in between.<sup>8–10</sup> The first dimensional (1st) column is usually coated with a non-polar stationary phase to separate gas analytes by their volatilities, whereas the second dimensional (2nd) column, usually relatively short, is coated with a polar stationary phase

to further separate gas analytes by their polarities. The modulator collects the effluent from the 1st column for a small fraction of the time, usually on the order of sub- to several seconds. Each fraction is re-focused into a very narrow band by the modulator and then sequentially injected into the 2nd column for additional separation. Since the modulator makes the separation at two columns independent, analytes can be differentiated from each other by their respective retention times at the 1st and the 2nd column, thus providing the 2-D separation information.

In spite of its enhanced separation capability, the conventional 2-D  $\mu$ GC suffers from several drawbacks such as a short modulation cycle time, which consumes a considerable amount of power and requires high performance for the modulator, and complicated re-construction of 2-D chromatograms, which requires extracting analytes' retention time at the 1st and the 2nd column from limited and isolated information.<sup>7,11</sup> The most significant limitation may be the short 2nd column,<sup>3</sup> as the 2nd separation must be completed within a modulation cycle (usually ranging from sub-second to

<sup>a</sup>Department of Biomedical Engineering, University of Michigan, 1101 Beal Avenue, Ann Arbor, Michigan 48109, USA. E-mail: [xsfan@umich.edu](mailto:xsfan@umich.edu)

<sup>b</sup>Center for Wireless Integrated Microsensing and Systems, University of Michigan, 1301 Beal Avenue, Ann Arbor, Michigan 48109, USA

<sup>c</sup>Department of Mechanical Engineering, University of Michigan, 2350 Hayward, Ann Arbor, Michigan, 48109, USA

<sup>d</sup>Department of Information Science & Electronic Engineering, Zhejiang University, 38 Zheda Road, Hangzhou, 310027, P. R. China

† Electronic supplementary information (ESI) available. See DOI: 10.1039/c2lc41159h

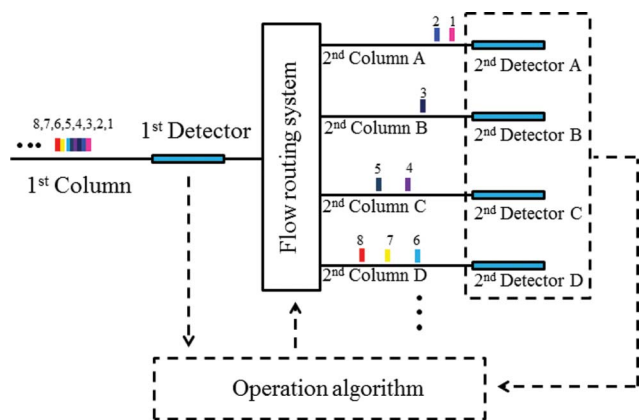


**Fig. 1** Schematic of a smart multi-channel 2-D  $\mu$ GC system. It consists of a 1st column, a flow routing system, multiple non-destructive on-column detectors and multiple independent 2nd columns, as well as a control/operation algorithm for automation. Dashed arrows and lines represent signal pathways. The 1st detector monitors the elution from the 1st column. When an entire elution peak passes the 1st detector, it is then sent to one of the 2nd columns for 2nd dimensional separation, which can be detected by the 2nd detectors. The operation algorithm receives the signal from the 1st detector and the 2nd detectors, and decides when to switch the flow routing system and to which of the 2nd columns the elution from the 1st column should be sent.

a few seconds) in order to avoid the potential wrap-around issue.<sup>3</sup> Consequently, the separation capability at the 2nd column is severely degraded.

We aim to develop a new 2-D  $\mu$ GC architecture to address the aforementioned problems. A general configuration of our proposed smart multi-channel 2-D  $\mu$ GC system, as illustrated in Fig. 1, consists of a 1st column, an on-column detector installed at the end of the 1st column to monitor the elution from the 1st column, a flow routing system to control connections between the 1st column and the 2nd columns, multiple independent 2nd columns, each of which has its own thermal injector and on-column detector, and a fully automated control/operation algorithm. The on-column detectors are non-destructive, do not affect the flow or separation, and introduce no additional dead volumes. During analysis, the gas mixture is first separated at the 1st column and the effluent is trapped by the thermal injector of one of the 2nd columns. Such processes are monitored in real-time by the 1st detector. Once an entire effluent peak comes out of the 1st column and is fully loaded onto the thermal injector, the injector is triggered to inject the trapped effluent into the 2nd column. This 2nd column is then registered as busy and is not assigned more effluent from the 1st column until the separation is completed (or after a certain pre-determined time lapse). Meanwhile, the flow routing system re-routes the subsequent effluent from the 1st column to another available 2nd column.

As compared to the conventional 2-D  $\mu$ GC, the smart multi-channel 2-D  $\mu$ GC architecture detects the effluents from the 1st column and makes the decision to route the effluent to one of the 2nd columns. Because of these unique designs, it has several distinct advantages.

(1) The entire effluent peak from the 1st column, instead of a slice of it, is sent to the 2nd column using a thermal injector. Consequently, our new  $\mu$ GC architecture eliminates the use of a thermal modulator having a short modulation cycle time, which is essential for the conventional 2-D  $\mu$ GC.<sup>5,12,13</sup> The repeated parsing of the 1st column effluent peak by a thermal modulator supposedly results in an increase in the peak capacity and sensitivity of 2-D GC analysis while retaining the original effluent order upon the transition between the two columns. However, a careful analysis and comparison with 1-D GC<sup>14</sup> indicate that real 2-D GC peak capacity cannot achieve the theoretical maximum  $n_1 \times n_2$ , where  $n_1$  and  $n_2$  are the peak capacities of the 1st and 2nd columns under optimal stand-alone conditions, respectively. The compromise of 2-D GC is attributed primarily to peak broadening of the 1st column effluents during the re-construction of their original peak profile after the modulation process. Our multi-channel 2-D  $\mu$ GC system does not suffer from the shortcomings inherently accompanying the short modulation cycle time of the thermal modulator, thus significantly reducing the broadening effect caused by re-construction of the original peak profile and power consumption in the analysis.

(2) All 2nd columns are independent of each other, and their coating, length, flow rate and temperature can be customized for best separation results. In particular, there is no more constraint on the upper limit of the 2nd column length (and separation time). Such flexibility is critical when long 2nd separation time is needed, thus significantly improving the 2nd separation.

(3) As the entire analyte (instead of a slice of it) within an effluent peak is sent into the 2nd column, the peak amplitude enhancement (the ratio between the analyte peak amplitude from the 1st column and that from the 2nd column)<sup>3</sup> and hence the system detection limit are considerably improved.

(4) This  $\mu$ GC architecture is highly scalable. More second dimensional columns can be added by simply using concatenated “Y” connectors or “1  $\times$  N” connectors. Higher dimensional separation (such as 3rd and 4th separation) can be introduced by connecting more columns to the outlet of each 2nd column. The corresponding illustrations are presented in Fig. S1, ESI.†

(5) Since the on-column detectors record the retention time of each elution peak at the corresponding column in real-time, construction of 2-D (or even higher dimensional) chromatograms can be greatly simplified.

Previously, we have demonstrated the smart multi-channel 2-D GC concept using conventional macro-scale components.<sup>15</sup> In this paper, we built a complete and automated smart multi-channel 2-D  $\mu$ GC system (see Fig. 2), which integrated a preconcentrator, micro-fabricated columns, on-column gas detectors, a flow routing system, thermal injectors and gas pumps, as well as an algorithm for control/operation of the system. We subsequently characterized and optimized this  $\mu$ GC system, and finally employed it in two important applications that highlight its uniqueness and advantages: (1) analysis of 31 workplace hazardous volatile organic com-

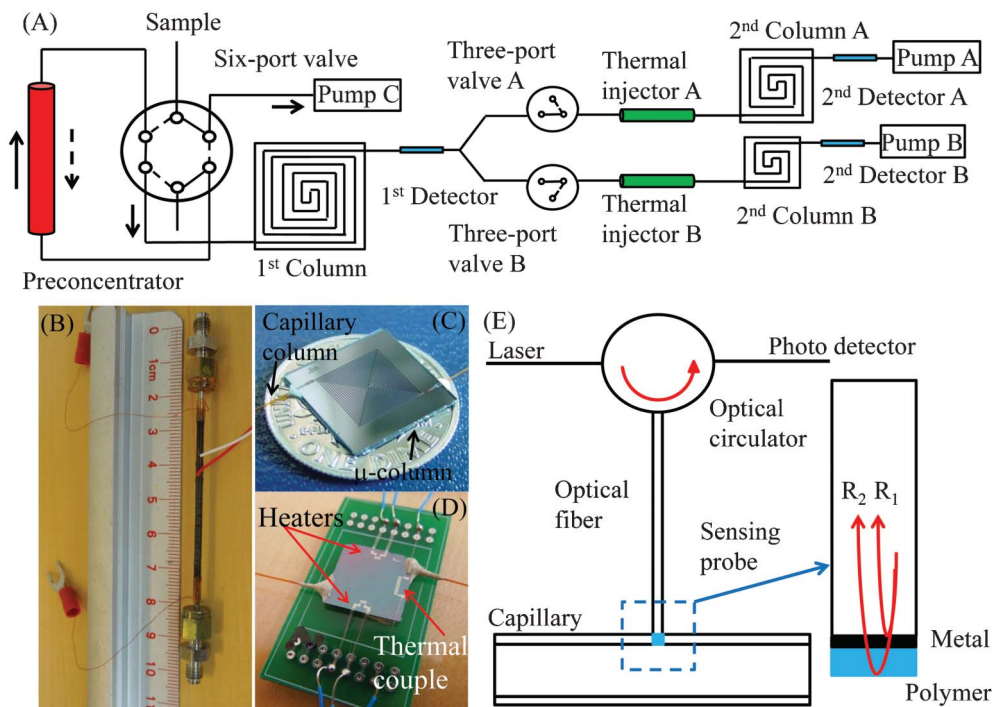


**Fig. 2** (A) Schematic of the proposed smart  $1 \times 2$  channel 2-D  $\mu$ GC with dual 2nd columns. A preconcentrator was connected to the 1st column through a six-port valve. During sampling (as shown by the dashed lines), sample was drawn into the preconcentrator by Pump C. During analysis (as shown by the solid lines), the trapped sample in the preconcentrator was released at high temperature and delivered onto the 1st column by a back-flush flow. The 1st column was connected to both 2nd columns by a Y-connector. Each of the 2nd columns had a three-port valve to control its connection with the 1st column. In this manner, the effluent from the 1st column was sent to the two 2nd columns alternately. (B) Photo of the preconcentrator. (C) Photo showing the front of the micro-fabricated column. (D) Photo showing the back of the micro-fabricated column. (E) Schematic of the on-column gas detector (the 1st and 2nd detectors were the same) using an optical fiber whose end-face was coated with a layer of vapor sensitive polymer.

pounds (VOCs) reported by California Standard Section 01350 Specification (Feb 2010 version 1.1)<sup>16</sup> and (2) rapid detection and identification of particular analytes out of the interference background.

## Experimental section

### Materials

All the analytes used in the experiment were purchased from Sigma (St. Louis, MO) and Fisher Scientific (Pittsburgh, PA). All analytes had purity greater than 97%. Guard columns (part no. 10000, i.d. = 250  $\mu$ m) were purchased from Restek (Bellefonte, PA). Carboxen 1018's (specific area = 675  $\text{m}^2 \text{g}^{-1}$ ) micro-porous carbon beads, which were used as the adsorbent materials of the preconcentrator, were purchased from Supelco (Bellefonte, PA). Universal quick seal column connectors (part no. 23627) and Universal angled "Y" connectors (part no. 20403-261) were purchased from Sigma and Restek, respectively. Single-mode fibers (SMF-28) were purchased from Corning (Corning, NY). The six-port valve (part no. EM2M76706) was purchased from Valco Instruments Co. Inc. (Houston, TX). Three-port valves (part no. 009-0269-900) and mini-diaphragm pumps (part no. D713-22-01) were purchased from Parker (Cleveland, OH). All materials were used as received.

### Experimental set-up

The schematic of the smart 2-D  $\mu$ GC is illustrated in Fig. 2. It included a preconcentrator, a six-port valve, a 1st Column, 1st Detector installed at the end of 1st Column, and two parallel 2nd columns: 2nd Column A and B, each of which was attached with a three-port valve, a thermal injector, 2nd Detector A or B and a gas pump. Note that to highlight the flexibility of the smart  $\mu$ GC two different lengths of the 2nd columns were used. Details of the major components of the system are described below.

### Preconcentrator

The preconcentrator was a stainless steel tube (0.318 cm i.d.) packed with 2.1 mg of Carboxen 1018 (sieved to  $\sim 200 \mu\text{m}$  in diameter (60/80 mesh)) held in place with a wire mesh and silanized glass wool (see Fig. 2(B)). It was preconditioned initially at 300  $^\circ\text{C}$  for 24 h under  $\text{N}_2$ . The preconcentrator was wrapped with an insulated copper heater wire and thermally desorbed at 300  $^\circ\text{C}$  for 5 min, which served to transfer the vapor mixture to the 1st column by the six-port valve actuation. A thermocouple was installed at the center of the preconcentrator to monitor its temperature in real-time. The capacity of the preconcentrator was verified in a separate series of tests, showing that the mass of each analyte trapped and transferred to the downstream GC matched that expected (within 1%).

### Micro-fabricated columns

The micro-fabricated column was fabricated by deep reactive ion etching a double spiral channel on a silicon substrate. A Pyrex 7740 glass slide was bonded anodically to the silicon substrate to seal the channel from the top (shown in Fig. 2(C)). The channel size was 240  $\mu\text{m}$  by 150  $\mu\text{m}$ . Two heaters and a thermocouple were embedded at the back of the chip for temperature ramping and monitoring, respectively (shown in Fig. 2(D)).

Two different stationary phases of non-polar OV-1 and polar OV-215 were used to coat the micro-fabricated columns. The coating procedures were as follows. (1) OV-1 solution was prepared by dissolving 22.3 mg OV-1 and 0.2 mg dicumyl peroxide in a 6 mL mixture of 1 : 1 (v : v) pentane and dichloromethane, whereas OV-215 solution was prepared by dissolving 20 mg OV-215 and 0.2 mg dicumyl peroxide in a 5 mL mixture of 1 : 4 (v : v) ether and ether acetate. (2) The micro-fabricated channel was filled with coating solution and held for 5 min. (3) The coating solution was evaporated from one end of the column by a vacuum pump, while the other end was sealed with a septum. (4) The coating was cross-linked to the inner wall of the column by ramping the column temperature from 160  $^{\circ}\text{C}$  to 180  $^{\circ}\text{C}$  at a rate of 0.2  $^{\circ}\text{C}$  min and staying at 180  $^{\circ}\text{C}$  for one hour. The resultant column coating had a uniform thickness of around 200 nm.

### On-column detectors

The fabrication detail of the on-column detector was discussed in our previous publications.<sup>17–19</sup> In this paper, a layer of gold (5 nm) and polydimethylsiloxane (PDMS) (2  $\mu\text{m}$ ) was sequentially deposited on the sensing probe. Light coupled in the sensing probe was partially reflected at the gold layer and the interface between the PDMS layer and air, generating a two beam interference spectrum. When the PDMS layer was exposed to gas analyte, its refractive index and/or thickness changed, resulting in the shift of the interference spectrum. By monitoring the interference spectrum shift, the quantitative and kinetic information of gas analytes was acquired. The sensing probe was then assembled with a short capillary column into an on-column detector, which can be easily connected to capillary separation columns through a universal quick seal column connector. An optical circulator was used to couple the light from a 1550 nm tunable diode laser into the sensing probe and redirect the reflected light into a photo detector.

### Thermal injector

The thermal injector was made of a quartz tube (i.d. = 2 mm, and 2 cm in length) packed with 6 mm long sorbent bed (Carbopack B and Tenax TA) held in place with silanized glass wool. Its outer surface was wrapped by an electrical coil for heating purposes. It was preconditioned at 300  $^{\circ}\text{C}$  under helium flow for one hour. The thermal injector can trap the effluent from the 1st column at room temperature and re-inject the trapped effluent onto the 2nd column when heated up to 300  $^{\circ}\text{C}$  within three seconds.

### Control/operation algorithm

A home-made LabView<sup>TM</sup> program was developed for automated control and operation of the system. It was based on our previous studies and characterization of the smart GC architecture using macro-scale components.<sup>15</sup> The operation procedures can be divided into three steps.

Step 1: 1st Column was connected to 2nd Column A and disconnected from 2nd Column B. The gas mixture was initially separated at 1st Column until 1st Detector detected a peak eluted out from 1st Column. When the entire eluted peak passed 1st Detector and was trapped by Thermal injector A at 2nd Column A, a signal was generated to trigger Three-port valve A to disconnect 2nd Column A from 1st Column and turn on Thermal injector A to inject the trapped analytes into 2nd Column A for further separation. The system then registered the status of 2nd Column A as “busy”. The “busy” status could be changed to “available” by a signal generated by 2nd Detector A when 2nd Column A completed separation or after certain pre-determined time lapse.

Step 2: When Three-port valve A disconnected 2nd Column A from 1st Column during operation of Step 1, 2nd Column B was connected to 1st Column. The remaining procedures were the same as in Step 1.

Step 3: When Three-port valve B disconnected 2nd Column B from 1st Column during operation of Step 2, the system inquired the status of 2nd Column A. If it was “available”, 2nd Column A was reconnected to 1st Column and the procedures in Step 1 were repeated. If it was “busy” (note that 2nd Column B is “busy” at this moment), both 2nd columns were disconnected from 1st Column and the separation at 1st Column was suspended, until one of the two 2nd columns became “available”, at which time the separation at 1st Column resumed and the effluent was sent to this “available” 2nd column.

Details of implementing the control/operation algorithm are described in the ESI.†

### Measurement

The gas sample was prepared by mixing target gas analytes and inertia nitrogen gas in a Tedlar bag (part no. 237-80, SKC Inc., Eighty Four, PA). The concentration of each gas analyte is listed in Table 1, which is the maximally allowable concentration reported by CA Section 01350.<sup>16</sup> The prepared gas sample was sampled by a preconcentrator through a six-port switching valve under a high flow rate of 50 mL min<sup>-1</sup> for 20 min. After sampling, the preconcentrator was heated up to 300  $^{\circ}\text{C}$  to release the sampled gas analytes by a back-flush flow. The mini-diaphragm pumps installed at the end of the 2nd columns delivered a flow rate of 1 mL min<sup>-1</sup>. Ultra high purity helium was used as the carrier gas. The temperature profiles of the 1st and the 2nd column and the thermal injectors were controlled by the LabView<sup>TM</sup> program. All other components were kept at room temperature.

## Results and discussion

### System characterization and optimization

The separation capability of a  $\mu\text{GC}$  system is affected by factors such as the stationary phase, column length and temperature

**Table 1** List of 31 workplace hazardous VOCs and their maximally allowable concentrations<sup>16</sup>

No.	Analyte name	Maximally allowable concentration (ng L <sup>-1</sup> )
1	Carbon disulfide	400
2	Dichloroethylene	35
3	Methyl <i>tert</i> -butyl ether	4000
4	Acetaldehyde	70
5	Methylene chloride	200
6	Chloroform	150
7	Hexane	3500
8	Dimethylformamide	40
9	Benzene	30
10	Carbon tetrachloride	20
11	Trichloroethylene	300
12	Dioxane	1500
13	Toluene	150
14	Vinyl acetate	100
15	Tetrachloroethylene	17.5
16	Ethylbenzene	1000
17	Ethylene glycol	200
18	Ethylene glycol monomethyl ether	30
19	Chlorobenzene	500
20	Ethylene glycol monoethyl ether	35
21	Isopropanol	3500
22	Methyl chloroform	500
23	Styrene	450
24	<i>m</i> -Xylene	350
25	Ethylene glycol monomethyl ether acetate	45
26	Propylene glycol monomethyl ether	3500
27	Formaldehyde	16.5
28	Ethylene glycol monoethyl ether acetate	150
29	Phenol	100
30	Dichlorobenzene	400
31	Isophorone	1000

ramping, *etc.* Optimization is needed before actual analysis to ensure that the system is well tuned to separate all components in the sample within a reasonably short amount of time. For the 2-D  $\mu$ GC, the system separation capability is determined by the separation capability of both the 1st and the 2nd column. The optimal separation is achieved when analytes

are sufficiently separated at both columns. In a conventional 2-D  $\mu$ GC system, optimization is usually accomplished through a trial-and-error process. In contrast, in our smart 2-D  $\mu$ GC system, the on-column detectors provide critical assessment of the separation capability of the 1st and the 2nd column.

To demonstrate this unique capability, a gas mixture containing six analytes (Analytes #15–#20 listed in Table 1) was used as the model system. We first implemented a system with one 1st column of 25 cm length and two 2nd columns of 50 cm and 25 cm length, respectively. Fig. 3(A) shows the real-time chromatograms obtained from this configuration. Apparently, significant co-elution occurred at 1st Column. Since the trigger signal was designed to be generated near the baseline, the entire co-eluted analytes (all six analytes in this particular case) were sent to 2nd Column A, resulting in insufficient separation of those analytes. The chromatograms provided by 1st Detector and 2nd Detector A allowed us to conclude that the above failure was due primarily to the insufficient separation of the analytes in the 1st column.

Once the cause of failure is identified, a number of methods are readily available to address this problem, such as changing the 1st column length, the 2nd column length, the flow rate or the temperature ramping profile. As a quick remedy, in our experiment we simply increased the length of the 1st column to 1 m, while keeping all other settings unchanged. As shown in Fig. 3(B), the gas mixture was separated into two (yet still co-eluted) peaks in the 1st column and all six analytes could be completely separated after the 2nd columns. It should be emphasized that such optimization is difficult to implement with the conventional 2-D  $\mu$ GC, as it is difficult to determine whether the insufficient 2-D separation is caused by the insufficient separation at the 1st column, the 2nd column or both.

### Analysis of 31 workplace hazardous VOCs

After optimization of our smart 2-D  $\mu$ GC system in the same manner as described previously, we employed it in analyzing 31 workplace hazardous VOCs reported by California Standard

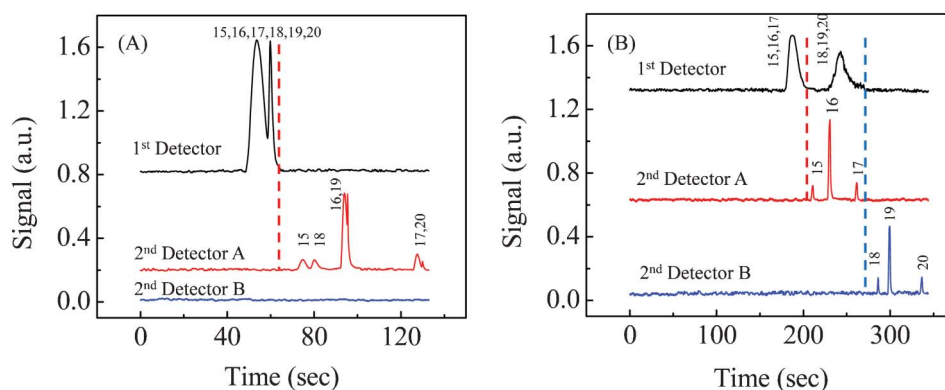


**Fig. 3** 2-D separation chromatograms obtained from the smart 2-D  $\mu$ GC illustrated in Fig. 2(A) under isothermal conditions at room temperature. The length of the 1st column was 0.25 m for (A) and 1 m for (B), respectively. The length of 2nd Column A and B were 0.5 m and 0.25 m, respectively, for both (A) and (B). (A) shows an insufficient 2-D separation before optimization, where co-elution occurred for Analyte #16 and #19, and for Analyte #17 and #20. Dashed line represents the time when separation started at 2nd Column A. (B) shows a sufficient 2-D separation after optimization. Dashed lines represent the time when separation started at 2nd Column A and B, respectively.

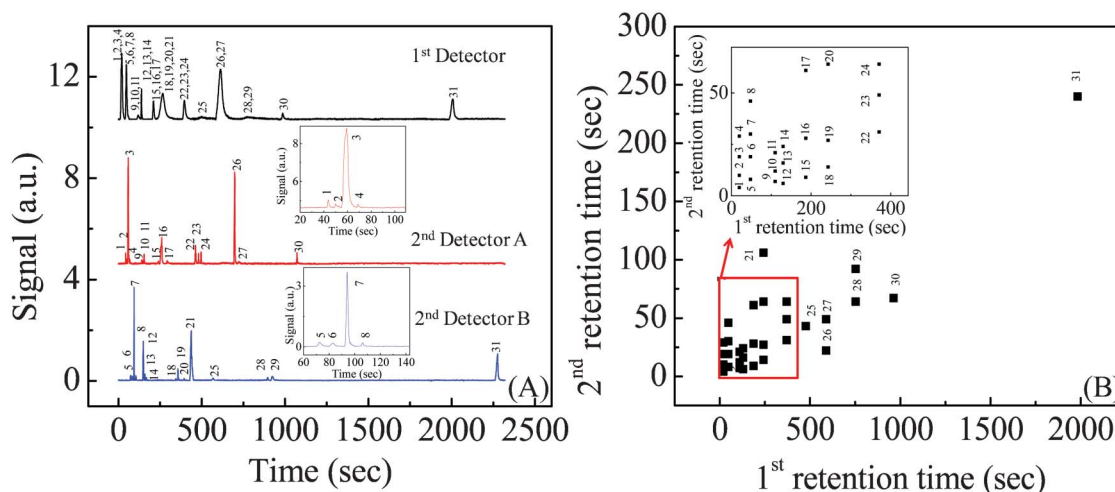


**Fig. 4** 2-D separation results of 31 workplace hazardous VOCs obtained from the 2-D  $\mu$ GC system shown in Fig. 2(A) under isothermal conditions at room temperature. (A) Real-time chromatograms from 1st Detector, 2nd Detector A and B. Curves are vertically shifted for clarity. Insets are enlarged parts from chromatograms at 2nd Column A and B, respectively. (B) The corresponding 2-D chromatogram extracted from (A). Detailed calculation method for the 1st and the 2nd retention time is presented in the ESI†. The 1st Column was 1 m long and was coated with OV-1. The 2nd Column A and B was 0.5 m and 0.25 m long, respectively. Both were coated with OV-215.

Section 01350 Specification (Feb 2010 version 1.1), which is the most popular US standard for evaluating and restricting indoor VOC emissions.<sup>16</sup> The name and the maximally allowable concentration of each analyte are listed in Table 1.

The first analysis was conducted under an isothermal condition at room temperature. As shown in Fig. 4(A), three real-time chromatograms were obtained from 1st Detector, 2nd Detector A and B, respectively. At 1st Column, 31 analytes were separated into 12 baseline-separated peaks, which were then sent to 2nd Column A and B alternately for further separation. Total analysis was completed within 38 min. Fig. 4(B) is the extracted 2-D chromatogram, from which we can observe a wide range of the retention times at the 2nd column up to approximately 4 min. Such long 2nd dimensional retention time would pose a significant challenge for a conventional 2-D  $\mu$ GC system due to the wrap-around issue,<sup>3</sup> whose maximal 2nd column separation time is limited by the short modulation cycle (ranging from sub-second to a few seconds).

To accelerate the analysis, temperature ramping was applied in this test. The 1st column was initially kept at 35 °C until the elution of the 11th peak at the 1st column, which was then heated up to 100 °C in 3 min. Both 2nd columns were kept at 45 °C during the whole analysis. Fig. 5(A) plots the three chromatograms from the 1st and two 2nd columns. Total analysis time was shortened to 20 min. Fig. 5(B) shows the extracted 2-D chromatogram. The longest 2nd dimensional retention time is approximately 110 s, which is still difficult to handle with the conventional 2-D  $\mu$ GC system.

#### Detection and identification of target analytes from interference background

In many applications, we are more interested in detection and identification of a particular target gas analyte or a set of analytes from interference background in a short time. In this

scenario, a complete separation of all components in a gas mixture may not be necessary. Rather, only the target analytes need to be separated out, which can greatly simplify the analysis procedures and shorten the analysis time.

To demonstrate such versatility of our  $\mu$ GC system, we used the same 31 VOCs, among which toluene and phenol were used as the target analytes and the remaining 29 VOCs served as the interference background. The system configuration was the same as used in Fig. 4(B). According to Fig. 4(B), the 1st and 2nd dimensional retention time of toluene (phenol) is 130 (753) seconds and 16 (92) seconds, respectively. Therefore, modifications were made in the LabView™ codes to define two time windows from 126 s to 136 s and from 720 s to 820 s, respectively, at the 1st dimension. If an effluent peak was detected within these two windows, the peak will be then sent to 2nd Column B for further separation/analysis. Any effluents outside these two windows were simply vented through 2nd Column A without conducting any further analysis. Note that the window at the 1st dimension can be very narrow (narrower than the elution peak) to ensure that most part of the target analyte is sent to the 2nd column while significantly rejecting interference background (even though they may co-elute with the target analyte). Therefore, the 2nd column separation becomes even easier, as fewer interferents are mixed in. At the 2nd dimension, 2nd Detector B identifies the peaks that have the same 2nd retention times as the target analytes.

As shown in Fig. 6, the 1st Detector detected an effluent peak within the 1st time window, which was sent to 2nd Column B for further separation. The 2nd Detector B then identified a peak that has the same 2nd retention time as toluene, indicating that toluene was contained in the gas mixture. Meanwhile, when the effluent in the 1st time window was analyzed at 2nd Column B, the separation at the 1st Column continued without interruption. The 1st Detector then detected another effluent peak within the 2nd time window,

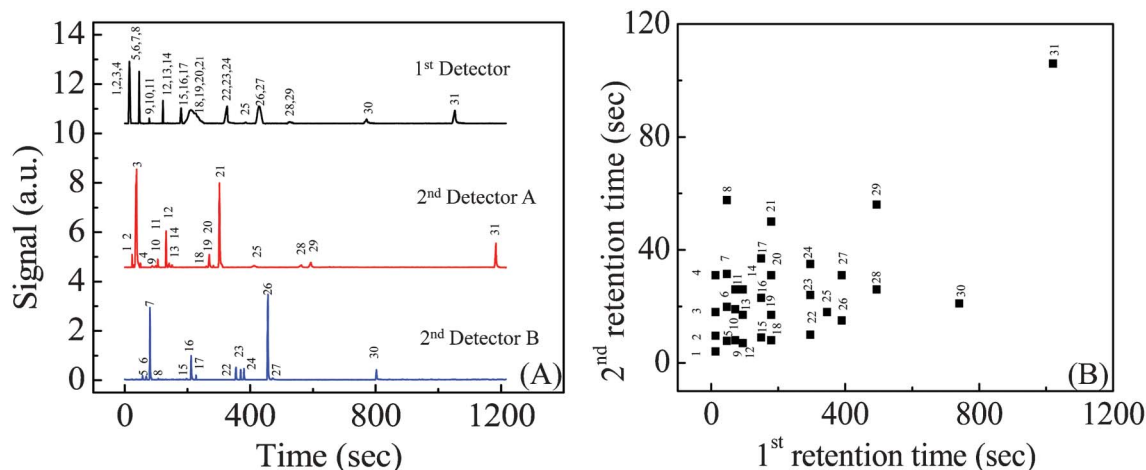


**Fig. 5** 2-D separation results of 31 workplace hazardous VOCs obtained from the smart 2-D  $\mu$ GC system shown in Fig. 2(A) with temperature ramping (other conditions were the same as in Fig. 4). (A) Real-time chromatograms from 1st Detector, 2nd Detector A and B. Curves are vertically shifted for clarity. (B) The corresponding 2-D chromatogram extracted from (A). Detailed calculation method for the 1st and the 2nd retention time is presented in the ESI.†

which was again sent to 2nd Column B for detection of phenol. Since no separation and analysis were conducted at 2nd Column A, the signal of 2nd Detector A is not present.

This detection and identification scenario is especially attractive for power hungry applications, such as remote autonomous monitoring, because it reduces the number of modulations for each analysis (no more than the number of the target analytes). When applied in the remote autonomous monitoring application, the system can be placed in the stand-by mode, only awakened by a suspicious peak(s) detected within the pre-determined window(s) at the 1st column.

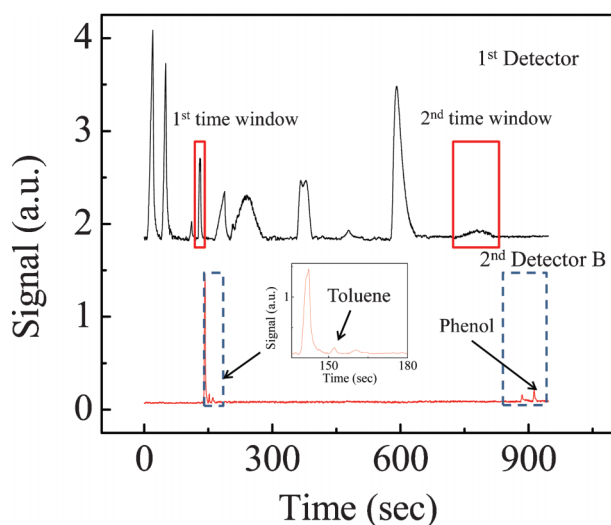


**Fig. 6** 2-D separation chromatograms obtained from the smart 2-D  $\mu$ GC shown in Fig. 2(A), when it was employed to detect toluene and phenol (as the target analyte) from interference background. Two time windows at the 1st dimensional separation were set to be from 126 s to 136 s and from 720 s to 820 s, respectively, as shown by the solid boxes. Dashed boxes show the 2nd dimensional separation of the effluents within the time windows defined by the solid boxes at the 1st dimension. Inset shows the enlarged first dashed box.

## Conclusion and future work

We have developed and built a complete smart multi-channel 2-D  $\mu$ GC system, and applied it in analyzing workplace hazardous VOCs, as well as specific detection of target analytes. Our results have shown that (1) the smart  $\mu$ GC can be used as a general-purpose gas analysis instrument having significantly enhanced second dimensional separation capability unattainable with the conventional 2-D  $\mu$ GC, and (2) it can be adapted for particular applications where only a set of target analytes need to be detected. Future work includes improving the operation algorithm to make the system smarter and more adaptive in control/operation, peak identification and trigger mechanism. The system will be further miniaturized by using micro-valves, micro-thermal injectors and on-chip on-column detectors.<sup>20–22</sup>

## Acknowledgements

The work is supported by the NSF (IOS 0946735) and the Center for Wireless Integrated Microsensing and Systems at the University of Michigan.

## References

- 1 J. J. Whiting, C. S. Fix, J. M. Anderson, A. W. Staton, R. P. Manginell, D. R. Wheeler, E. B. Myers, M. L. Roukes and R. J. Simonson, presented in part at the International Conference on Solid State Sensors and Actuators - Transducers, 2009, Denver, CO, June, 2009.
- 2 S. J. Kim, S. M. Reidy, B. P. Block, K. D. Wise, E. T. Zeller and K. Kurabayashi, *Lab Chip*, 2010, **10**, 1647–1654.
- 3 G. Serrano, D. Paul, S.-J. Kim, K. Kurabayashi and E. T. Zellers, *Anal. Chem.*, 2012, **84**, 6973–6980.

- 4 N. Oldridge, O. Panic and T. Górecki, *J. Sep. Sci.*, 2008, **31**, 3375–3384.
- 5 P. Q. Tranchida, D. Sciarrone, P. Dugo and L. Mondello, *Anal. Chim. Acta*, 2012, **76**, 66–75.
- 6 J. V. Seeley, *J. Chromatogr., A*, 2012, **1255**, 24–37.
- 7 Z.-D. Zeng, S.-T. Chin, H. M. Hugel and P. J. Marriott, *J. Chromatogr., A*, 2011, **1218**, 2301–2310.
- 8 J. Blomberg, P. J. Schoenmakers, J. Beens and R. Tijssen, *J. High Resolut. Chromatogr.*, 1997, **20**, 539–544.
- 9 J. Beens, H. Boelens, R. Tijssen and J. Blomberg, *J. High Resolut. Chromatogr.*, 1998, **21**, 47–54.
- 10 B. T. Weldegergis, A. M. Crouch, T. Górecki and A. de Villiers, *Anal. Chim. Acta*, 2011, **701**, 98–111.
- 11 S. E. Reichenbach, M. Ni, V. Kottapalli and A. Visvanathan, *Chemom. Intell. Lab. Syst.*, 2004, **71**, 107–120.
- 12 J. J. Whitting, C.-J. Lu, E. T. Zellers and R. D. Sacks, *Anal. Chem.*, 2001, **73**, 4668–4675.
- 13 M. Pursch, K. Sun, B. Winniford, H. Cortes, A. Weber, T. McCabe and J. Luong, *Anal. Bioanal. Chem.*, 2002, **373**, 356–367.
- 14 L. M. Blumberg, D. Frank, M. S. Klee and P. J. F. Sandra, *J. Chromatogr., A*, 2008, **1188**, 2–16.
- 15 J. Liu, M. K. Khaing Oo, K. Reddy, Y. B. Gianchandani, J. C. Schultz, H. M. Appel and X. Fan, *Anal. Chem.*, 2012, **84**, 4214–4220.
- 16 M. Horton, K. Belshe and A. Schwarzenegger, *Standard Method for the testing and evaluation of volatile organic chemical emissions from indoor sources using environmental chambers, Version 1.1*, California Department of Public Health, 2010.
- 17 J. Liu, Y. Sun and X. Fan, *Opt. Express*, 2009, **17**, 2731–2738.
- 18 J. Liu, Y. Sun, D. J. Howard, G. Frye-Mason, A. K. Thompson, S.-j. Ja, S.-K. Wang, M. Bai, H. Taub, M. Almasri and X. Fan, *Anal. Chem.*, 2010, **82**, 4370–4375.
- 19 J. Liu, N. K. Gupta, K. D. Wise, Y. B. Gianchandani and X. Fan, *Lab Chip*, 2011, **11**, 3487–3492.
- 20 J. H. Seo, J. Liu, X. Fan and K. Kurabayashi, *Anal. Chem.*, 2012, **84**, 6336–6340.
- 21 K. Reddy, Y. Guo, J. Liu, W. Lee, M. K. K. Oo and X. Fan, *Lab Chip*, 2012, **12**, 901–905.
- 22 K. Nachef, T. Bourouina, F. Marty, K. Danaie, B. Bourlon and E. Donzier, *J. Microelectromech. Syst.*, 2010, **19**, 973–981.